Check for updates

Follow-Up and Validation of K2 and TESS Planetary Systems With Keck NIRC2 Adaptive Optics Imaging

Joshua E. Schlieder[1]*, Erica J. Gonzales[2], David R. Ciardi[3], Rahul I. Patel[3],
Ian J. M. Crossfield[4], Justin R. Crepp[5], Courtney D. Dressing[6], Thomas Barclay[1,7] and
Andrew W. Howard[8]

[1] Exoplanets and Stellar Astrophysics Laboratory, NASA Goddard Space Flight Center, Greenbelt, MD, United States,
[2] Department of Astronomy and Astrophysics, University of California, Santa Cruz, Santa Cruz, CA, United States,
[3] Caltech/IPAC-NASA Exoplanet Science Institute, Pasadena, CA, United States, [4] Department of Physics and Astronomy,
University of Kansas, Lawrence, KS, United States, [5] Department of Physics, University of Notre Dame, Notre Dame, IN,
United States, [6] Astronomy Department, University of California, Berkeley, Berkeley, CA, United States, [7] University of
Maryland, Baltimore County, Baltimore, MD, United States, [8] Department of Astronomy, California Institute of Technology,
Pasadena, CA, United States

High resolution imaging (HRI) is a critical part of the transiting exoplanet follow-up and validation process. HRI allows previously unresolved stellar companions and background blends to be resolved, vetting false positive signals and improving the radii measurements of true planets. Through a multi-semester Keck NIRC2 adaptive optics imaging program, we have pursued HRI of K2 and TESS candidate planet host systems to provide the transiting exoplanet community with necessary data for system validation and characterization. Here we present a summary of our ongoing program that includes an up to date list of targets observed, a description of the observations and data reduction, and a discussion of planetary systems validated by the community using these data. This observing program has been key in NASA's K2 and TESS missions reaching their goals of identifying new exoplanets ideal for continued follow-up observations to measure their masses and investigate their atmospheres. Once processed, all observations presented here are available as calibrated images and resulting contrast curves through the Exoplanet Follow-up Observing Program (ExoFOP) website. We encourage members of the exoplanet community to use these data products in their ongoing planetary system validation and characterization efforts.

Keywords: adaptive optics—stars, binary stars, multiple stars, exoplanets, exoplanet candidates, exoplanet characterization

1. INTRODUCTION

The era of high-precision, space-based photometry to discover transiting exoplanets has led to a revolution in our understanding of planets beyond our solar system. NASA's *Kepler* mission (Borucki et al., 2010), which launched in 2009 and observed targets in a ∼115 sq. deg. part of the sky for nearly 4 years, identified ∼4,000 candidate transiting planets (Thompson et al., 2018). This sample allowed for ground breaking constraints on the statistical distribution and frequency of exoplanets (e.g., Dressing and Charbonneau, 2015; Fulton et al., 2017) and the discovery of many interesting individual systems (Lissauer et al., 2011; Quintana et al., 2014).

After hardware failures, the *Kepler* mission ended and the observatory was re-purposed as the K2 mission (Howell et al., 2014), a community driven, time domain photometry survey of 19 fields around the ecliptic plane. Compared to *Kepler*, K2 surveyed an order of magnitude more sky, accessed more diverse stellar populations, and observed a larger numberof bright targets amenable to follow-up observations. The exoplanet community has so far identified more than 1,300 candidate planets in K2 data (e.g., Kruse et al., 2019, and references therein). In this haul, K2 revealed small candidates transiting bright host stars suitable for detailed characterization (Crossfield et al., 2015; Montet et al., 2015) and allowed for additional statistical studies of the exoplanet population (Hardegree-Ullman et al., 2020). After the space craft expended its fuel in the Fall of 2018, it was no longer able to point precisely enough to perform science observations and the observatory was decommissioned.

The Transiting Exoplanet Survey Satellite (TESS, Ricker et al., 2015) launched in April 2018 and continues the *Kepler*/K2 transiting planet discovery legacy with a nearly all-sky survey. TESS observes in ~27 day Sectors and has so far obtained high precision photometric time-series over ≈80% of the sky to search for transiting planets. The mission aims to discover small planets around the closest brightest stars, leading to systems that are ideal for mass measurements and atmospheric characterization. So far, TESS has identified more than 3,000 candidate planets when those identified by the project (Guerrero and TESS Science Office, 2021) and the community[1] are taken into account. The mission is providing some of the most promising small planets for atmosphere characterization with the upcoming James Webb Space Telescope (JWST, e.g., Kostov et al., 2019).

An essential part of the process to confirm and characterize the ever increasing number of transiting exoplanet candidates is large scale, coordinated follow-up observations. Traditional confirmation of planet-like signals relies on precision radial velocity (PRV) spectroscopy to directly measure stellar reflex motion due to planets and derive planet masses. However, RV confirmation requires resource intensive long-term monitoring programs and may not be possible for faint targets and small planets due to signal-to-noise and expected RV amplitudes. In the majority of cases, a more tractable path to convert a candidate to a reliable planet requires follow-up to rule out sources of false positive signals (e.g., bound and background eclipsing binaries) with high statistical significance. Typical follow-up includes spectroscopy to determine the host star properties, lower precision RV screening for massive, short period companions, and imaging to identify bound companions and background sources. Statistical validation and dedicated follow-up has been used to rule out false-positives at high confidence for a large number of the *Kepler*, K2, and TESS candidates described previously. So far, approximately 2,400 *Kepler* candidates, more than 400 K2 candidates, and more than 100 TESS candidates have been validated or confirmed.

High spatial resolution imaging (HRI) has been critical to candidate exoplanet validation efforts. HRI has become the standard technique for detecting companion stars and background eclipsing binaries closer than 1″ and is a vital input for the statistical validation of small planets beyond the reach of RV observations. In addition to validation, HRI is crucial for measuring the true planetary radii and planet sizes by measuring the photometric blending of their hosts with bound and background stars (Ciardi et al., 2015). Here we describe a key program in a large HRI follow-up campaign to characterize K2 and TESS planetary systems. The program uses Keck NIRC2 adaptive optics (AO) imaging to discover and characterize close-in bound and background sources and provide the necessary data to validate high priority K2 and TESS targets, study exoplanet host star multiplicity, correct planetary radii for dilution from newly discovered companions, and place constraints on exoplanet demographics and occurrence rates. In subsequent sections we provide details on the construction of the program, our observations and analyses, and the results. We also discuss future plans with these data and, once processed, make available reduced data products for each observed target through the NASA Exoplanet Archive Exoplanet Follow-up Observing Program (ExoFOP) services for K2 and TESS. We encourage the exoplanet community to use these data in their ongoing analyses.

2. MATERIALS AND METHODS

2.1. Overview of the Observing Program

Following the need for HRI observations demonstrated with *Kepler* candidates and the transition to the community driven K2 mission, our team and collaborators undertook a large-scale effort to identify, follow-up, and validate K2 planet candidates (Crossfield et al., 2016, 2018; Dressing et al., 2017a,b, 2019; Livingston et al., 2018; Mayo et al., 2018; Petigura et al., 2018; Yu et al., 2018). As a key part of the follow-up campaign, we organized a multi-facility HRI program to observe and characterize K2 candidate exoplanet systems. As the K2 mission ended in 2018, the TESS mission began routine science operations and began delivering new exoplanet candidates. With this transition, we expanded our HRI follow-up program to pursue TESS targets through the TESS Follow-up Observers Program (TFOP).

Here we describe a portion of the K2 and TESS HRI program that was competitively pursued through the public NASA Keck time allocation[2]. We provide details on the NASA Keck observing programs allocated for these observations in **Table 1**. In the following sub-sections we describe our approaches to target selection, observations, data reduction, and analysis.

2.2. Target Selection

For the K2 aspect of the HRI program, we selected targets from the list of candidate exoplanet systems identified by this team and collaborators. The majority of these systems were identified in publicly available K2 data by our team using a multi-step process. K2 time-series were corrected for systematic errors introduced by the degraded pointing performance of the observatory using the `k2phot` software package[3]. Planet candidates were then

---

TABLE 1 | NASA Keck observing programs and nights.

Semester	ID #	UT Date	Weather	Notes
		2017-09-10	Clear skies	1/2 night
2017B	N213	2017-09-11	Clear skies	Full night
		2017-12-29	Clear skies	Full night
2018A	N119	2018-02-08	Fog, clouds	1/2 night
		2018-04-25	Clear skies	Full night
2018B	N214	2018-08-14	Clear skies	1/2 night
		2018-12-17	Clear skies	1/2 night
		2019-03-25	Clouds	1/2 night
2019A	N115	2019-04-07	Clear skies	1/2 night
		2019-06-09	Clear skies	1/2 night
2020A	N93	2020-05-28	Clouds	Full night

TABLE 2 | K2 targets and observation details[a].

EPIC ID	Semester	Date UT	Filter	T_{int} (s)	Coadds
201498078	2017B	2017-12-29	Br-γ	5	1
202071645	2017B	2017-12-29	Jcont	12	1
202071645	2017B	2017-12-29	Br-γ	10	1
202126852	2017B	2017-12-29	Jcont	4	1
202126852	2017B	2017-12-29	Br-γ	10	1
205916793	2017B	2017-09-11	Br-γ	20	1
206026136	2017B	2017-09-11	Br-γ	28	1
206155547	2017B	2017-09-11	K_p	11	1
206192335	2017B	2017-09-11	J	0.5	1
206192335	2017B	2017-09-11	Br-γ	6	1
210484192	2017B	2017-12-29	Jcont	10	1
210484192	2017B	2017-12-29	Jcont	5	1
210484192	2017B	2017-12-29	Br-γ	3	1
210484192	2018A	2018-02-08	Br-γ	1	1
210484192	2018A	2018-02-08	J	1	1
210508766	2017B	2017-12-29	K_p	45	1
210693462	2017B	2017-12-29	J	40	1
210693462	2018B	2018-12-17	Jcont	10	1
210693462	2017B	2017-12-29	K_p	20	1
210693462	2018B	2018-12-17	Br-γ	20	1

[a]This is a portion of the full table provided as an example of the format and content. The full table is available in electronic formation as **Supplementary Data Table 1**.

identified using the TERRA algorithm, adapted for use on K2 light curves from *Kepler* (Petigura et al., 2013). Diagnostic plots describing threshold crossing events (TCEs) were then visually vetted by a team of human volunteers to remove the most obvious false positives in the form of eclipsing binaries, stellar variability, and instrumental noise and produce lists of exoplanet candidates for each K2 campaign. Additional, community candidates identified using other systematics correction algorithms and planet search approaches were also considered. These included candidates resulting from the light curve detrending approaches described in Vanderburg and Johnson (2014), Aigrain et al. (2016), and Luger et al. (2016) and the planet searches described in Pope et al. (2016), Vanderburg et al. (2016), and Kruse et al. (2019). The combined potential targets were prioritized for Keck AO imaging follow-up on the basis of planet radius (planets ≤ 4 $R_\oplus$ were preferred), host star properties ($R_* < 1.5$ $R_\odot$, $V \lesssim$ 14 mag), and the planet's prospects as a future target for PRV mass measurements and transmission spectroscopy. This led to a total of 174 candidate K2 exoplanet systems being targeted in this program. The observed K2 targets and their observing parameters are provided in **Table 2**. This table is a portion of the full K2 target table and is provided as an example of the format and content. The full table is available in electronic formation as **Supplementary Data Table 1**.

The TESS aspect of the HRI program was organized through the TESS Follow-up Observing Program (TFOP)[4] and drew targets from the lists of exoplanet candidates publicly released by the TESS project. Building on the community driven, *ad-hoc* approach to follow-up from K2, TFOP was designed to prioritize and perform observations to go from a large sample of planet candidates (thousands) to a small sample of targets for PRV mass measurements ($\sim$100). Once transit-like events are identified in TESS 2-min cadence data by the Science Processing Operations Center (SPOC) mission pipeline (Jenkins et al., 2016) and in 30-min cadence data by the MIT Science Operations Center (SOC) Quick Look Pipeline (QLP), manual vetting of both SPOC and QLP transit events is performed by a dedicated

SOC team to provide a list of the most likely planet candidates. These candidates are then disseminated to the TFOP community for follow-up. The TESS observations presented here are part of TFOP Sub-Group 3 (SG3), which targets candidates with HRI to detect nearby sources unresolved by seeing limited observations ($\lesssim 1''$). The TESS mission began public releases of exoplanet candidates, called TESS Objects of Interest (TOIs), that fed into TFOP in September of 2018[5]. To select TESS targets for Keck AO imaging, we primarily considered TOI systems with small planets that would be most suitable for PRV follow-up to measure planet masses. This included selection on both the host star properties ($R_* < 1.5$ $R_\odot$, $V \lesssim$ 14 mag) and the candidate planets ($R_p \leq$ 4 $R_\oplus$). We also requested additional interesting TESS targets from the broader exoplanet community. This led to a total of 72 candidate TESS systems being targeted so far in this program. The observed TESS targets are detailed in **Table 3**. This table is a portion of the full TESS target table and is provided as an example of the format and content. The full table is available in electronic formation as **Supplementary Data Table 2**.

2.3. Observations

The observations described here cover nights in Keck semesters 2017B, 2018A, 2018B, 2019A, and 2020A; spanning the dates UT September 09 2017 to UT May 28 2020. The details of each observing run are provided in **Table 1**. In each of the observing runs, we used the NIRC2 instrument behind the

---

[4]https://tess.mit.edu/followup/

[5]https://tev.mit.edu/data/collection/193/

TIC ID	Semester	Date UT	Filter	T_{int} (s)	Coadds
13684720	2020A	2020-05-28	K	0.75	1
19025965	2019A	2019-03-25	Br-γ	15	1
19451711	2019A	2019-03-25	Jcont	0.4	50
19451711	2019A	2019-03-25	Br-γ	5	2
19451711	2019A	2019-03-25	Br-γ	1	2
19519368	2019A	2019-03-25	Br-γ	1	5
27649847	2019A	2019-04-07	Br-γ	15	1
31374837	2019A	2019-03-25	K	10	1
31374837	2019A	2019-03-25	K	1	20
33692729	2019A	2019-03-25	Br-γ	30	1
37770169	2019A	2019-03-25	K	1	30
71512186	2019A	2019-04-07	Br-γ	0.18	10
71512186	2019A	2019-04-07	Br-γ	0.18	50
73540072	2020A	2020-05-28	Br-γ	15	1
73540072	2020A	2020-05-28	Br-γ	20	1

[a]This is a portion of the full table provided as an example of the format and content. The full table is available in electronic formation as **Supplementary Data Table 2**.

TABLE 4 | NIRC2 filters used.

Filter	λ_c μm	Bandpass μm
Narrow band		
Kcont	2.2706	0.0296
Br-γ	2.1686	0.0326
Jcont	1.2132	0.0198
Broad band		
K	2.196	0.336
K_s	2.146	0.311
K_p	2.124	0.351
H	1.633	0.296
J	1.248	0.163

Natural Guide Star (NGS) AO system (Wizinowich et al., 2000) on the 10 m Keck-II telescope. The observations were obtained in a number of narrow and broad-band filters with central wavelengths near $\sim$2.2 μm to maximize the sensitivity to faint, low-mass companions. The exact choice of filter was dictated by the target NIR magnitude and the observing conditions (broader filters were used for fainter targets and in degraded conditions). If a potential companion was detected in quick look analyses, the target was also observed with shorter wavelength NIR filters, typically J-band, to facilitate companion color analyses. A full list of the NIRC2 filters used in this program is provided in **Table 4**. We used the narrow-angle mode of the camera to provide a pixel scale of 9.942 mas pixel^{-1} and a full field-of-view of 10$''$.

All of the observations in this program followed the standard dither set-up for NIRC2 observations that avoids the noisier lower-left quadrant of the detector. The observing sequences used a dither pattern with a step-size of 3$''$ that was repeated three times, with each dither offset 0.5$''$ from the previous, resulting in 9 frames. Integration times varied from <1 to 60 s per dither, depending on target NIR magnitudes, and typically used 1 coadd. Detailed information on the observations of each target are included in **Tables 2**, **3**.

2.4. Data Reduction and Analysis

All of the data in this program was reduced and analyzed using standard imaging approaches. The dithered science frames were dark corrected using calibration observations obtained each night. Sky frames were produced from the median average of the dithered science frames. Flats were produced from the median average of dark subtracted flat-field observations obtained each night. The science frames were then sky-subtracted and flat-fielded. The reduced frames where then combined into a single

image via an intrapixel interpolation scheme that co-aligns and median-coadds the frames while conserving flux. The final images are oriented with North up and East to left. Typical NIRC2 AO images obtained in good conditions have a resolution of $\sim$0.05$''$ (FWHM).

We estimated the sensitivity to these companions in each final, combined image by injecting simulated sources in 45$°$ azimuthal increments at discrete separations that were integer multiples of the central source's FWHM (following Furlan et al., 2017). To estimate the contrast sensitivity, the flux of each simulated source was increased until aperture photometry yielded a 5σ detection. The final contrast sensitivity as a function of separation was calculated by averaging all of the limits at that separation. Beginning approximately with the first TESS target observations in this program, we introduced contrast sensitivity uncertainties into our standard analyses. Uncertainties were estimated by measuring the RMS dispersion of the 5σ limits in each azimuthal annulus at each discrete separation. This process leads to contrast curves (in Δmag) for each target observation that represent the 5σ sensitivity limits of the imaging data as a function of separation from the central source. The NIRC2 observations typically yields NIR contrasts $\gtrsim$7 mag at 0.5$''$ separations, and $\gtrsim$4 mag at 0.1$''$ separations, providing access to faint, close-in companions (see e.g., Crossfield et al., 2016, their Figure 5).

3. RESULTS

After processing, the results of this observing program are made publicly available for community use on the NASA Exoplanet Archive's ExoFOP-K2[6] and ExoFOP-TESS[7] websites. For each observation we include: the reduced, combined images as FITS files, contrast curves as ASCII tables, and publication ready figures showing the contrast curve and final image as an inset.

---

[6]https://exofop.ipac.caltech.edu/k2/
[7]https://exofop.ipac.caltech.edu/tess/

FIGURE 1 | High-resolution images and 5σ contrast curves of stars hosting validated transiting exoplanets obtained in this Keck AO imaging program. **(A)** Br-γ observations of K2-266 (EPIC 248435473, Rodriguez et al., 2018). **(B)** Br-γ observations of K2-288 (EPIC 210693462, Feinstein et al., 2019). The observations revealed a faint companion to the southeast, K2-288B, that likely hosts the exoplanet. **(C)** K-band observations of TOI-421 (Carleo et al., 2020). **(D)** Br-γ observations of GJ 3473 (TOI-488). In **(C,D)**, the shaded regions represent the uncertainties in the contrast sensitivity estimates described in the text. Once processed, these contrast curves with reduced image insets are available for all targets observed in this program via the ExoFOP website. **(A–C)** are reproduced with permission of the AAS.
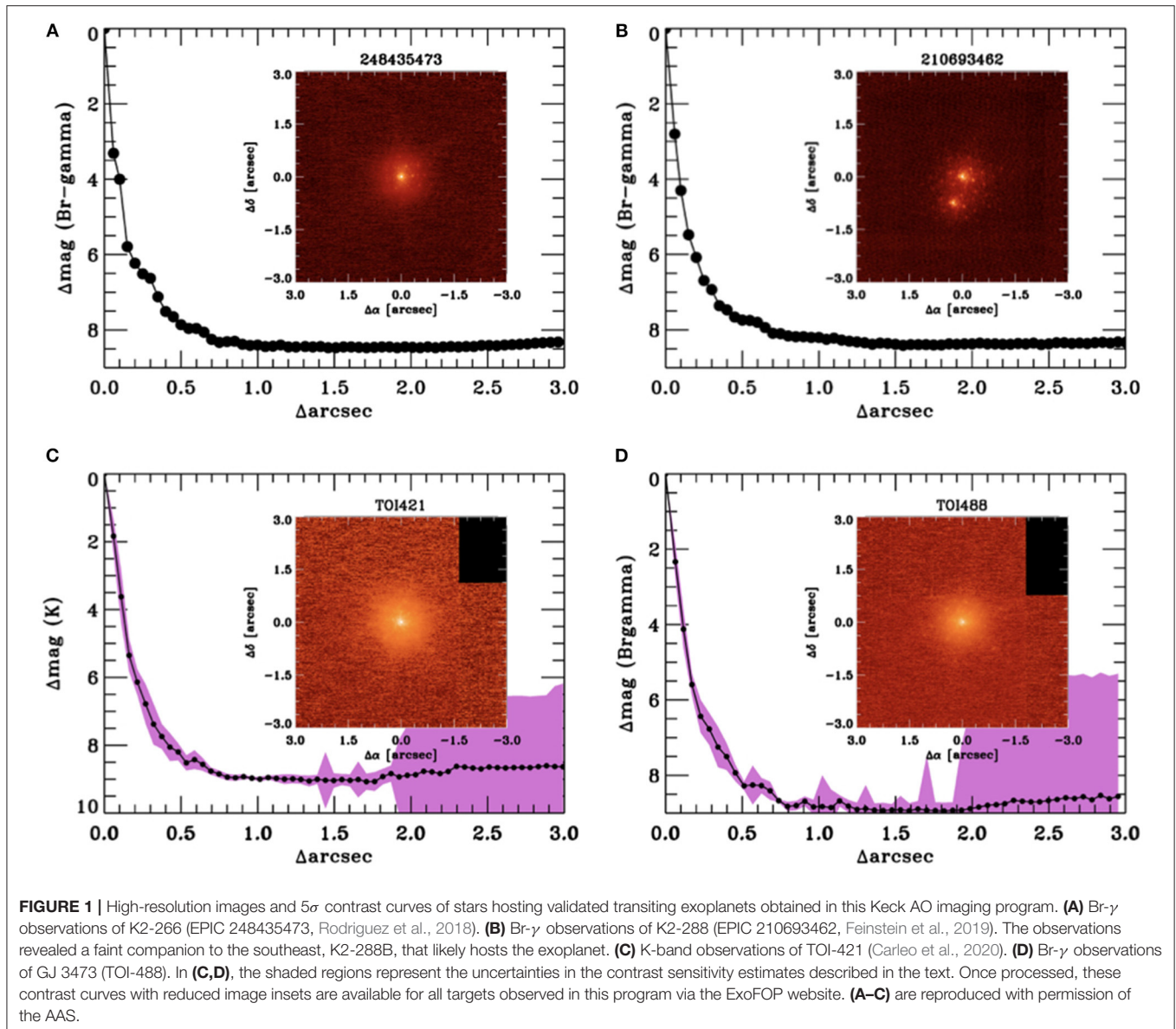
Figure 1 includes example reduced images and contrast curves from a selection of K2 and TESS targets in this program.

3.1. HRI in Planet Validation

The HRI data resulting from this observing program are key inputs to efforts to statistically validate transiting exoplanet candidates. HRI places deep constraints on the presence of bound and background sources in the vicinity of the presumed host stars that are blended in the much lower resolution images from *Kepler*/K2 and TESS used to produced light curves. These blended sources along the line of sight can host eclipsing binaries (EBs), that when diluted by the brighter primary source, mimic planet transits in the light curve. HRI is an observationally inexpensive and effective approach to mitigate contamination from blends.

The process of exoplanet validation systematically explores the large parameter space that could contain planet mimicking configurations and statistically constrain the probability. In practice, validation software combines light curve data, stellar properties, and observing constraints (i.e., contrast curves from HRI) with statistical priors on the likelihood of false positives. The aforementioned priors include simulations of the stellar population near the target and common false positive configurations (e.g., bound, background, and hierarchical EBs). The result of the validation analysis is the probability that a given transit signal is caused by one of the false positive scenarios explored or a true planet, the false positive probability (FPP). Validation is a powerful technique to confirm small planets beyond the reach of PRV measurements (like those in the habitable zone) and planets that orbit fainter stars. Several validation software packages have been developed and

used by the *Kepler*, K2, and TESS communities. These include BLENDER (Torres et al., 2011), PASTIS (Díaz et al., 2014), vespa (Morton, 2012, 2015), and TRICERATOPS (Giacalone and Dressing, 2020).

The HRI observations presented here, along with other complementary HRI observations from other Keck programs and other imaging facilities, have contributed to the validation of many hundreds of transiting exoplanet systems. For example, these data were key in the validation of many systems from the K2 mission. Some systems of note include K2-233, a young early-K dwarf hosting three small planets (David et al., 2018); K2-266, a K dwarf in a wide binary hosting at least four planets with one significantly misaligned (Rodriguez et al., 2018); and K2-288B, an M dwarf in a binary system hosting a small habitable-zone planet discovered by citizen scientists (Feinstein et al., 2019). The HRI observations of TESS targets are also beginning to validate and characterize systems around brighter, closer stars. This includes the TOI-421 system, three planets orbiting a bright G dwarf (Carleo et al., 2020); GJ 3473 (TOI-488), a nearby M dwarf hosting a hot, transiting, Earth-size planet (Kemmer et al., 2020), and TOI-503, a short period brown dwarf transiting an A type star (Šubjak et al., 2020).

4. DISCUSSION

The Keck HRI program described here and complementary observations with other facilities are ongoing and continue to secure time through the NASA Keck and other TACs. Future observations of high-priority TESS candidate planet hosts through TFOP SG3 will provide further characterizing data and progress the TESS mission toward its scientific goals via continued system validation. The data in hand will be included in forthcoming publications to present the full list of newly discovered companions and their properties, the multiplicity statistics of K2 and TESS planet host stars (e.g., Matson et al., 2018) and the effects of multiplicity on planetary systems (e.g., Kraus et al., 2016; Ziegler et al., 2018, 2020).

The observations will also be critical in future analyses of K2 and TESS exoplanet demographics and occurrence rates (e.g., Hardegree-Ullman et al., 2020; Zink et al., 2020). The HRI observations allow true planet radii to be included in these analysis. In the absence of HRI observations, planet radii could be underestimated due to dilution from unresolved, nearby sources that cause photometric blending of the transit (Ciardi et al., 2015; Furlan et al., 2017). Planet demographic and occurrence rates studies that do not account for these blends may overestimate the frequency of small planets. The inclusion of HRI data will improve our understanding of the true distributions and frequencies of planets across the Galaxy.

In addition to studies enabled directly by the HRI data, planetary systems validated and characterized in the context of HRI feed into further characterization efforts. This includes Doppler mass measurements and transmission and emission spectroscopy to detect planet atmospheres. These observations place direct constraints on the bulk compositions and chemical constituents of exoplanets. This is particularly true for the bright targets discovered by K2 and TESS that are most amenable to these measurements as we enter the era of extreme PRV observations and the JWST.

5. CONCLUSIONS

Here we summarized our multi-year campaign to observe K2 and TESS candidate exoplanet host stars using Keck NIRC2 AO imaging through the NASA Keck time allocation. The hundreds of targets we have observed continue to contribute to the validation of key new exoplanet systems and will be the focus of future studies delving into host star multiplicity and exoplanet occurrence rates. The TESS aspect of our program is ongoing through the TFOP consortium and will continue to provide HRI observations of high-priority candidate TESS systems. This includes ideal targets for further characterization to measure planet masses and study exoplanet atmospheres with current and future facilities. We encourage the exoplanet community to explore the calibrated and reduced data products we make available through ExoFOP and use these results in their validation and characterization efforts.

DATA AVAILABILITY STATEMENT

The Keck HRI datasets obtained through the described programs are publicly available from the Keck Observatory Archive (KOA) on a rolling basis following a proprietary period [https://www2.keck.hawaii.edu/koa/public/koa.php]. Once they are processed, the calibrated and reduced data products resulting from the described programs are publicly available from the ExoFOP websites for the K2 and TESS missions [https://exofop.ipac.caltech.edu/k2/ and https://exofop.ipac.caltech.edu/tess/].

AUTHOR CONTRIBUTIONS

JS led the manuscript, produced the tables and figure, performed the observations, and wrote the NASA Keck proposals. EG contributed to the text and tables, performed the observations, and wrote the NASA Keck proposals. DC contributed to the text, tables, and figure, performed the data reduction, produced the publicly available data products, and performed the observations. RP and IC contributed to the text and performed the observations. JC, CD, TB, and AH contributed to the text. All authors contributed to the NASA Keck proposals that led to the described data.

FUNDING

ACKNOWLEDGMENTS

telescope time allocated to the National Aeronautics and Space Administration through the agency's scientific partnership with the California Institute of Technology and the University of California. The Observatory was made possible by the generous financial support of the W. M. Keck Foundation. The authors recognize and acknowledge the significant cultural role and reverence that the summit of Maunakea has always had within the indigenous Hawaiian community.

We were most fortunate to conduct observations from this mountain.

SUPPLEMENTARY MATERIAL

The Supplementary Material for this article can be found online at: https://www.frontiersin.org/articles/10.3389/fspas.2021.628396/full#supplementary-material

REFERENCES

Aigrain, S., Parviainen, H., and Pope, B. J. S. (2016). K2SC: flexible systematics correction and detrending of K2 light curves using Gaussian process regression. *Mon. Not. RAS* 459, 2408–2419. doi: 10.1093/mnras/stw706

Borucki, W. J., Koch, D., Basri, G., Batalha, N., Brown, T., Caldwell, D., et al. (2010). Kepler planet-detection mission: introduction and first results. *Science* 327:977. doi: 10.1126/science.1185402

Carleo, I., Gandolfi, D., Barragán, O., Livingston, J. H., Persson, C. M., Lam, K. W. F., et al. (2020). The multiplanet system TOI-421. *Astron. J.* 160:114. doi: 10.3847/1538-3881/aba124

Ciardi, D. R., Beichman, C. A., Horch, E. P., and Howell, S. B. (2015). Understanding the effects of stellar multiplicity on the derived planet radii from transit surveys: implications for Kepler, K2, and TESS. *Astrophys. J.* 805:16. doi: 10.1088/0004-637X/805/1/16

Crossfield, I. J. M., Ciardi, D. R., Petigura, E. A., Sinukoff, E., Schlieder, J. E., Howard, A. W., et al. (2016). 197 Candidates and 104 validated planets in K2's first five fields. *Astrophys. J. Suppl.* 226:7. doi: 10.3847/0067-0049/226/1/7

Crossfield, I. J. M., Guerrero, N., David, T., Quinn, S. N., Feinstein, A. D., Huang, C., et al. (2018). A TESS dress rehearsal: planetary candidates and variables from K2 campaign 17. *Astrophys. J. Suppl.* 239:5. doi: 10.3847/1538-4365/aae155

Crossfield, I. J. M., Petigura, E., Schlieder, J. E., Howard, A. W., Fulton, B. J., Aller, K. M., et al. (2015). A nearby M star with three transiting super-earths discovered by K2. *Astrophys. J.* 804:10. doi: 10.1088/0004-637X/804/1/10

David, T. J., Crossfield, I. J. M., Benneke, B., Petigura, E. A., Gonzales, E. J., Schlieder, J. E., et al. (2018). Three small planets transiting the bright young field star K2–233. *Astron. J.* 155:222. doi: 10.3847/1538-3881/aabde8

Díaz, R. F., Almenara, J. M., Santerne, A., Moutou, C., Lethuillier, A., and Deleuil, M. (2014). PASTIS: Bayesian extrasolar planet validation–I. General framework, models, and performance. *Mon. Not. RAS* 441, 983–1004. doi: 10.1093/mnras/stu601

Dressing, C. D., and Charbonneau, D. (2015). The occurrence of potentially habitable planets orbiting M dwarfs estimated from the full Kepler dataset and an empirical measurement of the detection sensitivity. *Astrophys. J.* 807:45. doi: 10.1088/0004-637X/807/1/45

Dressing, C. D., Hardegree-Ullman, K., Schlieder, J. E., Newton, E. R., Vanderburg, A., Feinstein, A. D., et al. (2019). Characterizing K2 candidate planetary systems orbiting low-mass stars. IV. Updated properties for 86 cool dwarfs observed during campaigns 1–17. *Astron. J.* 158:87. doi: 10.3847/1538-3881/ab2895

Dressing, C. D., Newton, E. R., Schlieder, J. E., Charbonneau, D., Knutson, H. A., Vanderburg, A., et al. (2017a). Characterizing K2 candidate planetary systems orbiting low-mass stars. I. Classifying low-mass host stars observed during campaigns 1–7. *Astrophys. J.* 836:167. doi: 10.3847/1538-4357/836/2/167

Dressing, C. D., Vanderburg, A., Schlieder, J. E., Crossfield, I. J. M., Knutson, H. A., Newton, E. R., et al. (2017b). Characterizing K2 candidate planetary systems orbiting low-mass stars. II. Planetary systems observed during campaigns 1–7. *Astron. J.* 154:207. doi: 10.3847/1538-3881/aa89f2

Feinstein, A. D., Schlieder, J. E., Livingston, J. H., Ciardi, D. R., Howard, A. W., Arnold, L., et al. (2019). K2–288Bb: a small temperate planet in a low-mass binary system discovered by citizen scientists. *Astron. J.* 157:40. doi: 10.3847/1538-3881/aafa70

Fulton, B. J., Petigura, E. A., Howard, A. W., Isaacson, H., Marcy, G. W., Cargile, P. A., et al. (2017). The California-Kepler survey. III. A gap in the radius distribution of small planets. *Astron. J.* 154:109. doi: 10.3847/1538-3881/aa80eb

Furlan, E., Ciardi, D. R., Everett, M. E., Saylors, M., Teske, J. K., Horch, E. P., et al. (2017). The Kepler follow-up observation program. I. A catalog of companions to Kepler stars from high-resolution imaging. *Astron. J.* 153:71. doi: 10.3847/1538-3881/153/2/71

Giacalone, S., and Dressing, C. D. (2020). triceratops: A tool for rapid validation of *TESS* objects of interest and application to 424 planet candidates. *arXiv* 2002.00691.

Guerrero, N., and TESS Science Office (2021). "TESS objects of interest catalog in the TESS prime mission and beyond," in *American Astronomical Society Meeting Abstracts, Volume 53 of American Astronomical Society Meeting Abstracts*, 117.01.

Hardegree-Ullman, K. K., Zink, J. K., Christiansen, J. L., Dressing, C. D., Ciardi, D. R., and Schlieder, J. E. (2020). Scaling K2. I. Revised parameters for 222,088 K2 stars and a K2 planet radius valley at 1.9 $R_{\oplus}$. *Astrophys. J. Suppl.* 247:28. doi: 10.3847/1538-4365/ab7230

Howell, S. B., Sobeck, C., Haas, M., Still, M., Barclay, T., Mullally, F., et al. (2014). The K2 mission: characterization and early results. *Publ. ASP* 126:398. doi: 10.1086/676406

Jenkins, J. M., Twicken, J. D., McCauliff, S., Campbell, J., Sanderfer, D., Lung, D., et al. (2016). *The TESS Science Processing Operations Center, Volume 9913 of Society of Photo-Optical Instrumentation Engineers (SPIE) Conference Series*, 99133E. doi: 10.1117/12.2233418

Kemmer, J., Stock, S., Kossakowski, D., Kaminski, A., Molaverdikhani, K., Schlecker, M., et al. (2020). Discovery of a hot, transiting, earth-sized planet and a second temperate, non-transiting planet around the M4 dwarf GJ 3473 (TOI-488). *arXiv* 2009.10432. doi: 10.1051/0004-6361/202038967

Kostov, V. B., Schlieder, J. E., Barclay, T., Quintana, E. V., Colón, K. D., Brande, J., et al. (2019). The L 98–59 system: three transiting, terrestrial-size planets orbiting a nearby M dwarf. *Astron. J.* 158:32. doi: 10.3847/1538-3881/ab2459

Kraus, A. L., Ireland, M. J., Huber, D., Mann, A. W., and Dupuy, T. J. (2016). The impact of stellar multiplicity on planetary systems. I. The ruinous influence of close binary companions. *Astron. J.* 152:8. doi: 10.3847/0004-6256/152/1/8

Kruse, E., Agol, E., Luger, R., and Foreman-Mackey, D. (2019). Detection of hundreds of new planet candidates and eclipsing binaries in K2 campaigns 0–8. *Astrophys. J. Suppl.* 244:11. doi: 10.3847/1538-4365/ab346b

Lissauer, J. J., Fabrycky, D. C., Ford, E. B., Borucki, W. J., Fressin, F., Marcy, G. W., et al. (2011). A closely packed system of low-mass, low-density planets transiting Kepler-11. *Nature* 470, 53–58. doi: 10.1038/nature09760

Livingston, J. H., Crossfield, I. J. M., Petigura, E. A., Gonzales, E. J., Ciardi, D. R., Beichman, C. A., et al. (2018). Sixty validated planets from K2 campaigns 5–8. *Astron. J.* 156:277. doi: 10.3847/1538-3881/aae778

Luger, R., Agol, E., Kruse, E., Barnes, R., Becker, A., Foreman-Mackey, D., et al. (2016). EVEREST: pixel level decorrelation of K2 light curves. *Astron. J.* 152:100. doi: 10.3847/0004-6256/152/4/100

Matson, R. A., Howell, S. B., Horch, E. P., and Everett, M. E. (2018). Stellar companions of exoplanet host stars in K2. *Astron. J.* 156:31. doi: 10.3847/1538-3881/aac778

Mayo, A. W., Vanderburg, A., Latham, D. W., Bieryla, A., Morton, T. D., Buchhave, L. A., et al. (2018). 275 Candidates and 149 validated planets orbiting bright stars in K2 campaigns 0–10. *Astron. J.* 155:136. doi: 10.3847/1538-3881/aaadff

Montet, B. T., Morton, T. D., Foreman-Mackey, D., Johnson, J. A., Hogg, D. W., Bowler, B. P., et al. (2015). Stellar and planetary properties of K2 campaign 1 candidates and validation of 17 planets, including a planet receiving earth-like insolation. *Astrophys. J.* 809:25. doi: 10.1088/0004-637X/809/1/25

Morton, T. D. (2012). An efficient automated validation procedure for exoplanet transit candidates. *Astrophys. J.* 761:6. doi: 10.1088/0004-637X/761/1/6

Morton, T. D. (2015). *VESPA: False Positive Probabilities Calculator*. Astrophysics Source Code Library, record ascl:1503.011.

Petigura, E. A., Crossfield, I. J. M., Isaacson, H., Beichman, C. A., Christiansen, J. L., Dressing, C. D., et al. (2018). Planet candidates from K2 campaigns 5–8 and follow-up optical spectroscopy. *Astron. J.* 155:21. doi: 10.3847/1538-3881/aa9b83

Petigura, E. A., Marcy, G. W., and Howard, A. W. (2013). A plateau in the planet population below twice the size of earth. *Astrophys. J.* 770:69. doi: 10.1088/0004-637X/770/1/69

Pope, B. J. S., Parviainen, H., and Aigrain, S. (2016). Transiting exoplanet candidates from K2 campaigns 5 and 6. *Mon. Not. RAS* 461, 3399–3409. doi: 10.1093/mnras/stw1373

Quintana, E. V., Barclay, T., Raymond, S. N., Rowe, J. F., Bolmont, E., Caldwell, D. A., et al. (2014). An earth-sized planet in the habitable zone of a cool star. *Science* 344, 277–280. doi: 10.1126/science.1249403

Ricker, G. R., Winn, J. N., Vanderspek, R., Latham, D. W., Bakos, G. Á., Bean, J. L., et al. (2015). Transiting exoplanet survey satellite (TESS). *J. Astron. Telesc. Instr. Syst.* 1:014003. doi: 10.1117/1.JATIS.1.1.014003

Rodriguez, J. E., Becker, J. C., Eastman, J. D., Hadden, S., Vanderburg, A., Khain, T., et al. (2018). A compact multi-planet system with a significantly misaligned ultra short period planet. *Astron. J.* 156:245. doi: 10.3847/1538-3881/aae530

Šubjak, J., Sharma, R., Carmichael, T. W., Johnson, M. C., Gonzales, E. J., Matthews, E., et al. (2020). TOI-503: the first known brown-dwarf Am-star binary from the TESS mission. *Astron. J.* 159:151. doi: 10.3847/1538-3881/ab7245

Thompson, S. E., Coughlin, J. L., Hoffman, K., Mullally, F., Christiansen, J. L., Burke, C. J., et al. (2018). Planetary candidates observed by Kepler. VIII. A fully automated catalog with measured completeness and reliability based on data release 25. *Astrophys. J. Suppl.* 235:38. doi: 10.3847/1538-4365/aab4f9

Torres, G., Fressin, F., Batalha, N. M., Borucki, W. J., Brown, T. M., Bryson, S. T., et al. (2011). Modeling Kepler transit light curves as false positives: rejection of blend scenarios for Kepler-9, and validation of Kepler-9 d, a super-earth-size planet in a multiple system. *Astrophys. J.* 727:24. doi: 10.1088/0004-637X/727/1/24

Vanderburg, A., and Johnson, J. A. (2014). A technique for extracting highly precise photometry for the two-wheeled Kepler mission. *Publ. ASP* 126:948. doi: 10.1086/678764

Vanderburg, A., Latham, D. W., Buchhave, L. A., Bieryla, A., Berlind, P., Calkins, M. L., et al. (2016). Planetary candidates from the first year of the K2 mission. *Astrophys. J. Suppl.* 222:14. doi: 10.3847/0067-0049/222/1/14

Wizinowich, P., Acton, D. S., Shelton, C., Stomski, P., Gathright, J., Ho, K., et al. (2000). First light adaptive optics images from the Keck II telescope: a new era of high angular resolution imagery. *Publ. ASP* 112, 315–319. doi: 10.1086/316543

Yu, L., Crossfield, I. J. M., Schlieder, J. E., Kosiarek, M. R., Feinstein, A. D., Livingston, J. H., et al. (2018). Planetary candidates from K2 campaign 16. *Astron. J.* 156:22. doi: 10.3847/1538-3881/aac6e6

Ziegler, C., Law, N. M., Baranec, C., Howard, W., Morton, T., Riddle, R., et al. (2018). Robo-AO Kepler survey. V. The effect of physically associated stellar companions on planetary systems. *Astron. J.* 156:83. doi: 10.3847/1538-3881/aace59

Ziegler, C., Tokovinin, A., Briceño, C., Mang, J., Law, N., and Mann, A. W. (2020). SOAR TESS survey. I. Sculpting of TESS planetary systems by stellar companions. *Astron. J.* 159:19. doi: 10.3847/1538-3881/ab55e9

Zink, J. K., Hardegree-Ullman, K. K., Christiansen, J. L., Petigura, E. A., Dressing, C. D., Schlieder, J. E., et al. (2020). Scaling K2. III. Comparable planet occurrence in the FGK samples of campaign 5 and Kepler. *Astron. J.* 160:94. doi: 10.3847/1538-3881/aba123